



This is a repository copy of *Deflected versus preshaped soft pneumatic actuators: A design and performance analysis toward reliable soft robots.*

White Rose Research Online URL for this paper:

<https://eprints.whiterose.ac.uk/176027/>

Version: Accepted Version

Article:

Perez Guagnelli, E.R. and Damian, D. orcid.org/0000-0002-0595-0182 (2022) Deflected versus preshaped soft pneumatic actuators: A design and performance analysis toward reliable soft robots. *Soft Robotics*, 9 (4). pp. 713-722. ISSN 2169-5172

<https://doi.org/10.1089/soro.2020.0119>

Final publication is available from Mary Ann Liebert, Inc., publishers
<http://dx.doi.org/10.1089/soro.2020.0119>.

Reuse

Items deposited in White Rose Research Online are protected by copyright, with all rights reserved unless indicated otherwise. They may be downloaded and/or printed for private study, or other acts as permitted by national copyright laws. The publisher or other rights holders may allow further reproduction and re-use of the full text version. This is indicated by the licence information on the White Rose Research Online record for the item.

Takedown

If you consider content in White Rose Research Online to be in breach of UK law, please notify us by emailing eprints@whiterose.ac.uk including the URL of the record and the reason for the withdrawal request.



eprints@whiterose.ac.uk
<https://eprints.whiterose.ac.uk/>

Deflected vs Pre-shaped Soft Pneumatic Actuators: A Design and Performance Analysis Towards Reliable Soft Robots

Eduardo Perez-Guagnelli¹ and Dana D. Damian¹

Abstract—Soft Pneumatic Actuators (SPAs) are customizable and conformable devices that enable desired motions in soft robots. Interactions with the environment or handling during their fabrication could introduce defects into SPAs that affect their performance. These defects could lead to high-stress concentrations in the SPAs body and heterogeneous, unrepeatable, or inconsistent expansion affecting their reliability. In this work, we aim to improve the reliability of soft robots by modeling and characterizing the performance of SPAs with widely used chamber shapes and cross-sectional geometries under variable loading conditions. We also compare their capacity to provide homogeneous, repeatable and time-wise consistent expansion with low-stress concentrations and provide a set of principles for the design of reliable SPAs. Expansion of SPAs with Straight chambers demonstrated to be more repeatable, with an average deviation of 0.06 mm and showed more than a thousand times less stress than any other chamber types. The expansion of pre-shaped SPAs with Helical chambers showed to be up to 500% more homogeneous and 300% more efficient than their deflected counterparts. SPAs with squared cross-sectional geometries displayed more than a 1000 times more time-wise consistent expansion over their circular counterparts. We conclude that SPAs that retain less potential energy or are less affected by its effects are more reliable. We derive these results into a set of principles for the design of reliable SPAs. These principles offer solutions to make informed decisions prior to fabrication to mitigate the most common reliability problems for SPAs and soft robots.

I. INTRODUCTION

Soft robots are machines made of lightweight and highly compliant materials that can be customized to perform a wide range of functions such as locomotion [1] or gripping [2]. Given their compliance, hyperelasticity and inherent safety, soft robots are well-suited to be used in applications such as exoskeletons [3] and implants [4]. Soft actuators are the building blocks of soft robots that enable their motion. Currently, most of them are actuated fluidically and fabricated out of elastomeric matrices with embedded rigid or semi-rigid materials [5]. Design of soft pneumatic actuators (SPAs) has been based on four approaches: (1) variation of cross-sectional geometry [6], (2) morphology of the pneumatic chamber [7], (3) fiber-reinforcements variation [8] or (4) hybrid rigid-soft interactions [9]. Given their influence in motion and considering that some SPAs are designed to perform precise tasks such as minimally invasive surgery [10], it is essential to comprehend how the design of soft actuators impacts soft robots reliability.

Similar to other mechanical meta-materials [11], interaction with the environment or handling during their assembly or fabrication could introduce defects into the SPAs that impact their performance. These defects could lead to high stress concentrations in the SPAs body reducing their fatigue life [12] and efficiency reduction as a consequence of unwanted deformations [13]. Those unwanted deformations cause heterogeneous expansion of the SPAs. It is frequently assumed that SPAs expand homogeneously throughout its unconstrained areas. The oversight of heterogeneous expansion makes it difficult to predict the SPAs performance accurately. Additionally, neglecting repeatability and time-wise consistency of expansion in highly precise tasks could cause serious damage, for example, a burst or leak in a clinical treatment.

Different approaches have been considered to make soft actuators with robust performance. Robertson, *et al* [14] demonstrated that bundled fiber-reinforced SPAs are robust enough to be able to maintain their capacity even when the air supply is cut off to its individual SPAs. Miron and Plante [12] proposed design principles to improve fatigue life of extensible pneumatic muscles, for example, the use of reinforcements to provide low-friction interactions to avoid abrasion between two rubber surfaces that might lead to failure. Martinez, *et al* [15] characterized elastomeric pneumatic structures that can have their functions restored after mechanical damage is applied. Although these approaches provide relevant insights into the design of more reliable SPAs, there is no systematic approach on the impact of chamber design, cross-sectional geometry and fabrication methods as a triad that might be affecting the performance of SPAs. Additionally, although different cross-sectional and chamber geometries have been tested for the design of SPAs, the analysis of their performance under loaded conditions has been done as part of a more complex or constrained system, possibly inadvertently hiding possible underlying effects of the chambers alone. In this work, a combination of modeling, experimental characterization and statistical analysis is used to analyze the design of widely used SPAs, delivering the following contributions: (1) reliability quantification of different SPAs designs by deriving their amount of expansion under variable loading conditions and deflections, (2) a comparative study among different SPA designs based on their performance reliability and (3) a set of principles for the design and fabrication of reliable SPAs. By implementing these design principles derived from our systematic analysis into the planning and design of soft systems, roboticists will be able to make informed decisions into the development of

¹Department of Automatic Control and Systems Engineering, University of Sheffield, UK. d.damian@sheffield.ac.uk This work was partially funded by The United Kingdom Engineering and Physical Sciences Research Council (EPSRC) Tissue-RIMOTE grant [EP/S021035/1] and The National Council of Science and Technology of Mexico (CONACYT).

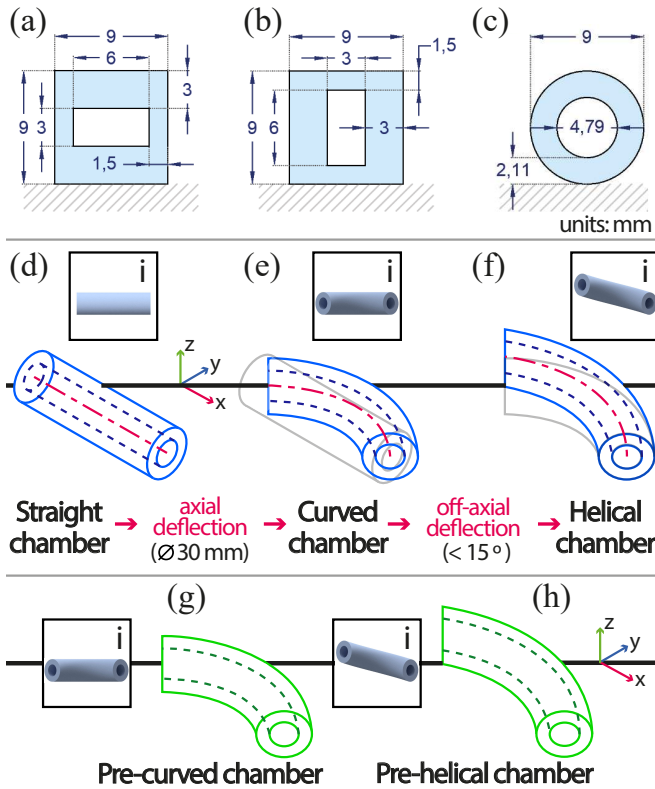


Fig. 1. The tested SPA samples of differing cross-sectional geometries and chamber designs. (a) Dimensions of the Horizontal, (b) Vertical and (c) Circular cross-sectional geometries. These geometries were used for each type of chamber: (d) Straight, (e) Curved, (f) Helical, (g) Pre-curved and (h) Pre-helical chambers. Chambers (e) and (f) are shaped by manually deflecting Straight chambers around a cylinder that works as an environmental constraint (Fig. 3). Pre-shaped chambers (d,g,h) have been molded under their respective shapes, meaning there is no manual deflection involved in shaping and placing them around the environmental constraint. Inserts i in figures d-h show a frontal view of their respective chambers for clarity.

more accurate, robust and efficient robots, increasing their performance predictability and potentially making it easier to model and replicate their motions.

II. SPAS DESIGN

We investigated a series of SPAs designs by varying their geometrical properties such as their pneumatic chamber 3D shape, either this shape is obtained by deflecting a chamber or by pre-configuring it from the molding stage, and their cross sectional geometry.

A. Pneumatic Chamber 3D Shape

We selected three of the most used 3D shapes in the design of SPAs: Straight (Fig. 1(d)), Curved (Fig. 1(e)) and Helical (Fig. 1(f)). The Straight chamber is the most common shape for pneumatic chambers, typically used for single [16] or multi-chamber linear actuators that curve when pressurized [17]. We designate a Curved chamber if it has been initially straight and an axial deflection curved it as a consequence of pressurization or manipulation (Fig. 1(e)). Typical examples of the use of Curved chambers are grippers [18]. If the chamber was fabricated curved, meaning that no deflection

TABLE I
SPAS VARIATIONS COMBINING DIFFERENT CROSS-SECTIONAL GEOMETRIES AND CHAMBER 3D SHAPES

Chamber Shape	Cross-Sectional Geometry		
	Horizontal	Vertical	Circular
Deflected	Horizontal Curved	Vertical Curved	Circular Curved
Helical	Horizontal Helical	Vertical Helical	Circular Helical
Pre-shaped	Horizontal	Vertical	Circular
Straight	Horizontal Straight	Vertical Straight	Circular Straight
Pre-curved	Horizontal Pre-curved	Vertical Pre-curved	Circular Pre-curved
Pre-Helical	Horizontal Pre-Helical	Vertical Pre-Helical	Circular Pre-Helical

force has been inputted to the structure to modify its shape, it will be referred to as Pre-curved (Fig. 1(g)). We designate a Helical chamber if it has been initially straight and then axial and off-axial deflections coiled it as consequence of pressurization or manipulation (Fig. 1(f)). If the chamber was fabricated coiled meaning that no deflection force has been inputted to the structure to modify its shape, it will be referred to as Pre-helical (Fig. 1(h)). Some examples include biomimetic grippers [19], [20], walking helically-arranged tubes [21] and soft implantable devices [4]. Due to their versatility, these three shapes of chamber design, deflected or pre-shaped can be found in one system, for instance, in modules with different motion capabilities [22], [13].

B. Cross-Sectional Geometry

It has been demonstrated that varying certain design parameters in the cross-sectional geometry of a soft actuator has an impact on its performance. For example, by varying its wall thickness, the actuator will expand in the regions with lowest stiffness [23]. Additionally, the force generated by the pressure acting on the soft walls that resist expansion is highly dependant on the cross-sectional area [8]. The height-width ratio of the chamber and air channel will also affect the resistance of the actuator to physical instabilities. For this reason, we decided to explore the implications of orientation of two identical SPAs with anisotropic wall thickness (Fig. 1(a,b)). Considering these design parameters and given that Squared and Circular geometries are the most found in the literature, we selected the cross-sectional geometries Horizontal (Fig. 1(a)), Vertical (Fig. 1(b)) and Circular (Fig. 1(c)) to be investigated in this study. For the design of the SPAs with a circular cross-sectional geometry we prioritized to keep consistent (with the squared SPAs) the cross-sectional area of the air channel (18 mm^2) and their maximum height (9 mm). In summary, combining the selected chamber types described in Section II-A and the cross-sectional geometries shown in Fig. 1(a-c), we analyzed the performance of 15 different SPAs (Table I). The cross-sectional area and length of the air channel was kept consistent among designs.

C. SPAs Response to Mechanical Instabilities

When disturbed by loads, SPAs behavior will vary depending on their response to instabilities. The SPA that buckles at lower critical loads will have its chamber shape deformed

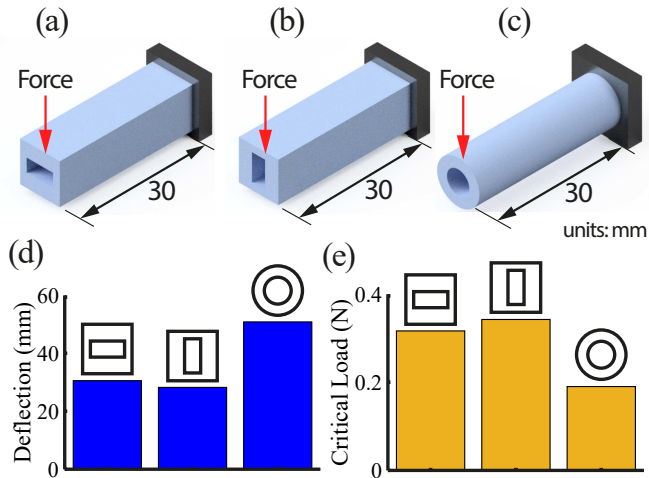


Fig. 2. Preliminary analysis of the SPAs response to mechanical instabilities per cross-sectional geometries. (a) Cantilever beams used in this analysis for the Horizontal, (b) Vertical and (c) Circular Straight SPAs. (d) Deflection and (e) Critical load response for each Straight SPA. The dimensions of the cross-sectional geometries are shown in Fig. 1(a-c)

by lower weights, potentially affecting its performance. Also, an SPA that shows a higher displacement in comparison to other SPAs that have been deflected under the same loads will retain less potential energy. In order to assure the selection of SPAs designs with different structural capabilities that we can compare under various scenarios, we assessed analytically the three cross-sectional geometry designs. We calculated the mechanical response of Straight Horizontal (Fig. 2(a)), Vertical (Fig. 2(b)) and Circular (Fig. 2(c)) SPAs to deflection using the Euler-Bernoulli tip deflection formula:

$$\delta = \frac{FL^3}{3EI} \quad (1)$$

where δ is the deflection of the chamber, F is the deflection force, L is the length of the SPA, E is the Young's Modulus of the silicone and I is the second moment of area of the cross-section.

To identify the mechanical resistance of the SPAs to buckling we identified their critical load using the Euler's buckling theory:

$$F = \frac{n^2\pi^2EI}{L^2} \quad (2)$$

where L is the length of the SPA, E is the Young's Modulus of the silicone, I is the second moment of area of the cross-section and n is a constant for buckling of cantilever-like beams. Although equations (1) and (2) do not consider the hyperelasticity of the material, they are a linearization of the behavior of the chambers for small loads that works as a simple way to verify the SPAs response to instabilities.

In Fig. 2(d), we can see that the Circular Straight chamber deflects more than the Squared Chambers. However, the Vertical Straight chamber has the highest critical load in comparison to the Circular one (Fig. 2 (e)). In both cases, Horizontal and Vertical performed similarly, showing that

a change in orientation might produce also a different performance in our following experiments. Additionally, we confirmed that some of the SPAs have more resistance to buckling but less to deflecting. These values will be further discussed against experimental results in Section V.

III. METHODS

In this work, we analyze the performance of deflected and pre-shaped SPAs that have been submitted to variable loading conditions prior to pressurization to determine their reliability to provide a set of design principles for the development of reliable SPAs. In this section, first we describe the fabrication process of the SPAs. Second, we define the reliability requirements and assessment metrics for the analysis of the SPAs performance. Third, we predict expansion differences among the three SPAs with different cross-sectional geometries using Finite Element Modeling (FEM) in order to validate our experimental setup and FEM settings calibration. Fourth, we introduce the experimental protocol and setup we used to evaluate the SPAs. Fifth, we selected highly reliable SPAs and conducted a stress analysis using FEM in order to identify stress concentrations that might lead to failure. Finally, we conducted a statistical analysis to determine if the variation of cross-sectional geometries and chamber shapes have a significant impact into their expansion. The electronic control platform is described in [24].

A. Fabrication

ABS 3D Printed molds (Stratasys Mojo TM) were used to cast the chambers and caps of the actuators. Ecoflex 00-30 (Smooth On Inc.) was mixed and defoamed (ThinkyTM ARE-250 Mixer) and then poured into the molds (Fig. 3(a)). Prior to casting the chambers, we sprayed the interior of the molds using a release agent (Mann @, Ease-Release 200). This avoids the chambers sticking to the molds and allows them to be removed without damage. Then, we cured them at room temperature for three hours. Next, we thermally post-cured them at 80° for two hours and then at 100° for one hour.

B. Reliability Requirements

In this study, we assess the reliability of 15 different SPAs based on their maximum expansion after being loaded and pressurized under identical conditions. The identification of the variables Fd and Δa in the setup is shown in Figs. 3(b,c) and Figs. 3(d,e) respectively. We identified the following as relevant performance requirements and metrics for the design and evaluation of highly reliable SPAs (Fig. 4):

1) *Repeatability*: When pressurized, the SPAs should expand consistently every cycle, provided that pressure and loading conditions are identical. We quantified repeatability of each SPA by calculating the standard deviation (SD) of each group of trials ($\sigma^0, \sigma^1, \sigma^2, \sigma^3$ in Fig. 4) under the same loading conditions (Fd). Then, we calculated the inverse of the average of all σ ($\bar{\sigma}$) to obtain an index of SPAs repeatability (Rp).

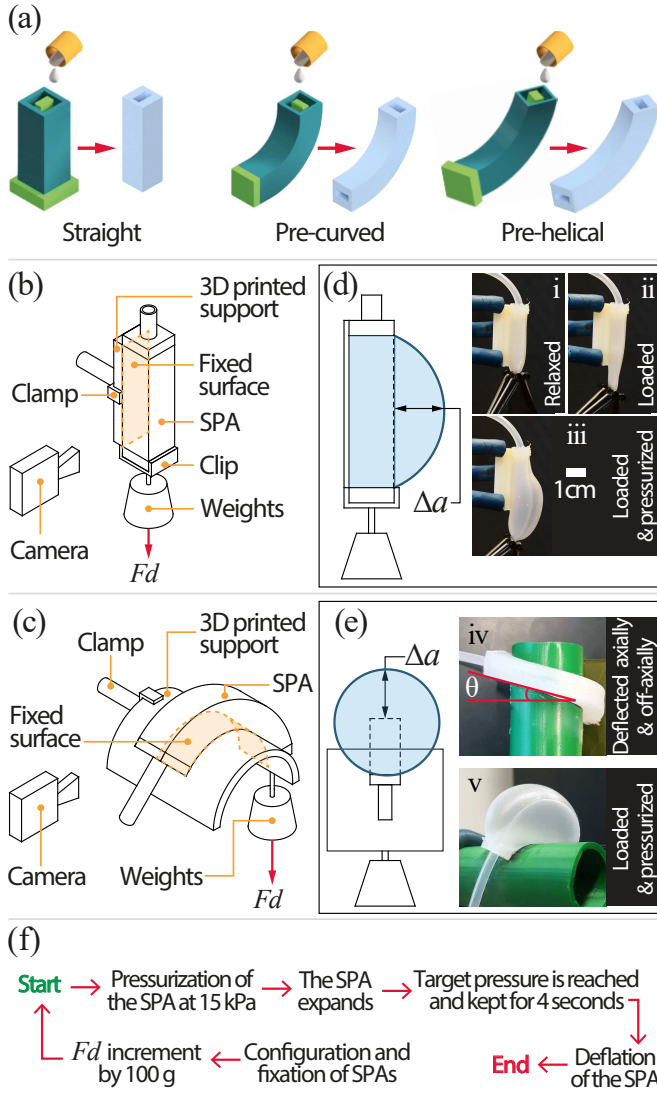


Fig. 3. Experimental setup and protocol. (a) Fabrication molds for casting of the SPAs. Similar molds were used to cast all the different cross-sectional geometries. (b) Isometric-view diagram of Straight and (c) non-straight SPAs, identifying the setup parts and loads (Fd). (d) Identification of Δa as the maximum expansion of Straight and (e) non-Straight SPAs. Inserts i-iii show different Straight SPAs' states, iv shows angle Θ , set to 15° for Helical and Pre-helical chambers and v shows a Pre-helical chamber loaded and pressurized. Angle Θ is kept to 0° for Curved and Pre-curved chambers. (f) Experimental procedure. We conducted experiments where Fd was 0, 100, 200 and 300 g.

2) **Robustness**: When pressurized, the SPAs should expand consistently every cycle, provided that pressure conditions are identical, regardless of loading conditions varying. The higher the heterogeneity (H) of expansion, the lower the robustness. To quantify robustness of the SPAs we used the following equation:

$$R_b = \frac{1}{H} \quad (3)$$

Where H represents the heterogeneity of expansion as a consequence of loading introduced into the SPA, defined by the SD of all the maximum expansion measurements ($\Delta a^{0.1} \dots \Delta a^{1.5}$) across all loading conditions (Fd). A highly

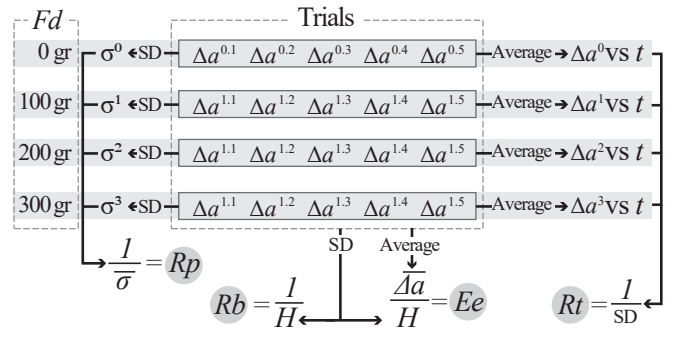


Fig. 4. Calculation of performance metrics for the reliability analysis of SPAs

(R_p) Repeatability, (R_b) Robustness, (E_e) Efficient Expansion and (R_t) Reiteration. Fd is the loading force. SD is standard deviation. H is heterogeneity of expansion. Experimental parameters of Fd and Δa are identified in Fig. 3(b).

robust SPA will show low Heterogeneity (H) values and consequently, a high robustness value (R_b).

3) **Expansion Efficiency**: When pressurized, the SPAs should show high levels of expansion (Δa) with low heterogeneity (H). Inefficient expansion is represented by either, high expansion rates with high heterogeneity, low expansion with low heterogeneity or low expansion with high heterogeneity. We determined the efficiency of expansion of the SPAs by using the following equation:

$$E_e = \frac{\bar{\Delta a}}{H} \quad (4)$$

Where $\bar{\Delta a}$ is the average of Δa across all loading conditions (Fd) and H is the heterogeneity of expansion (Fig. 4).

4) **Reiteration**: When pressurized, the SPAs should reach their maximum expansion, in the same amount of time every cycle, provided that pressure conditions are identical, despite variations in the loading conditions (Fd).

To evaluate reiteration performance of SPAs, we correlated the time they take to reach Δa^0 , Δa^1 , Δa^2 and Δa^3 and the time they take to reach the target pressure plus 4 seconds. This additional time helps us to verify that the expansion pressure has reached equilibrium. A highly reiterative SPA will reach Δa^0 , Δa^1 , Δa^2 and Δa^3 under the same amount of time every cycle.

C. Expansion Prediction Using FEM

To predict expansion differences due to the varied cross-sectional geometries, we developed an FEM of the Horizontal, Vertical and Circular geometries with Straight chamber shape. Afterwards, we validated our models by comparing Δa (Fig. 3(b)) of the simulations with experimental data. We selected these SPA designs as a baseline for comparison with other SPAs as they are the most basic configuration for a pneumatic actuator. We developed the 3D models of the SPAs on Fusion360 (Autodesk[®]) and then, imported them into Abaqus/CAE (Simulia, Dassault SystemesTM). The SPAs models were meshed using quadratic tetrahedral, 3D

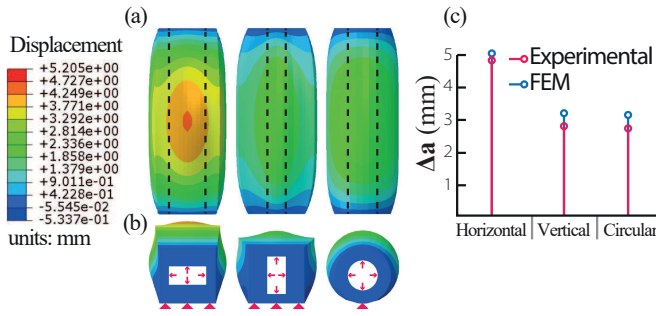


Fig. 5. Finite Element Analysis of the three different cross-sectional geometries in Straight SPAs upon pressurization at 15 kPa. (a) Top view showing displacement contours and (b) Front cross-sectional view showing load and boundary conditions. (c) FEM predictions and experimental results comparison.

solid hybrid elements (C3D10H). To capture the hyperelastic behavior of silicone, we used the Ogden material model, which parameters are described in [25]. Boundary conditions and loads are represented in Fig. 5(b).

D. SPAs Reliability Characterization

We fixed Pre-curved and Pre-helical SPAs around a rigid 3D printed supporting tube with a diameter of 30 mm using cyanoacrylate adhesive (Fig. 3(d)). For the Curved and Helical SPAs, we fixed the proximal end of the SPA to the supporting tube and then we manually deflected it and glued it until obtaining the desired shape, following a guiding line drawn prior the adhesion. For the Helical and Pre-helical SPAs we rotated the 3D printed tube 15° to avoid the gravity force to affect the coiling angle which is also 15° (Fig. 3(e) ii). For the other SPAs, this angle was kept at 0°. For the Straight SPAs, we used a flat 3D printed support and equally fixed them using cyanoacrylate adhesive (Fig. 3(b)). The 3D printed supports simulate environmental constraints and by gluing the lower surfaces of the SPAs to these supports we simulate inextensible layers in common SPAs. After the pre-shaped and deflected configurations were fixed, we placed a clip at the distal section of the SPAs to hang weights from them. We added those weights incrementally to serve as variable loads, from 0 to 300 g (Fd in Fig. 3(b,d)). These weights represent the loads that could be exerted into the system by the designer or the environment during fabrication or actuation. Afterwards, we pressurized and expanded the chamber at 15 kPa. We recorded and measured the maximum expansion Δa (Fig. 3(c,e)) using an image processor (ImageJ, NIH). We conducted five trials per experiment. A diagram of the experimental protocol is shown in (Fig. 3(f)).

E. Stress Analysis

To provide a more complete understanding of the SPAs behavior and its possible impact in loading-related scenarios, we identified stress concentrations in their hyperelastic material as a response to expansion that might lead to failure of the SPAs by developing a static stress numerical analysis. To do this, after performing the reliability assessment of

the different SPA designs (Fig. 7), we selected the three SPAs with the highest expansion efficiency (Ee) per cross-sectional geometry. Since it is a measure of reliability based on heterogeneity and expansion (H and $\bar{\Delta}a$ in Fig. 4) which are metrics of reliability frequently used in soft robotics, we decided to base our analysis on efficiency of expansion (Ee). Then, we contrasted and analyzed the stress differences between our baseline (Section III-C) and the SPAs with highest Ee values Fig. 4(c)). The parameters and settings used in this numerical analysis are described in Section III-C.

F. Statistical Analysis

To determine if the difference in expansion among SPAs is significant, we conducted a statistical analysis, where the maximum expansion $\bar{\Delta}a$ is the dependent variable. First, we ran a Shapiro-Wilk normality test to verify if the data is normally distributed. Since it was not normally distributed and given that geometry and chamber shape are two independent variables with more than one variation, we proceeded to conduct a Kruskal-Wallis test with a *Bonferroni* correction and a P -value = 0.05.

IV. EXPERIMENTAL RESULTS

A. FEM Experimental Validation

There was a good agreement between modeling and experimental results for the expansion of the Straight SPAs (Fig. 5). These results validated our experimental setup and FEM settings calibration. Additionally, this works as a benchmark for comparisons over more complex conditions, as in the stress analysis presented in Section IV-C.

B. Reliability Characterization

Fig. 6 shows that there are important differences in the performance of the SPAs with different cross-sectional geometry, shape and degree of deflection. For example, the robustness of the Vertical cross-sectional geometry is lower in a Straight chamber (Fig. 6(a)) than in a Pre-helical chamber (Fig. 6(e)), meaning that the Vertical Pre-helical SPA expansion is more consistent than the Vertical Straight Chamber regardless of the loading (Fd) conditions. Results for all the SPAs will be further discussed in Section V-D. Based on the SPAs performance represented in Fig. 6 and using the metrics defined in Section III-B we proceeded to assess all the SPAs based on their repeatability, robustness, expansion efficiency and reiteration.

1) *Repeatability*: Fig. 7(a) shows a rapid decrease in repeatability, starting from Horizontal Straight down to most of the Circular geometries. Repeatability of the maximum expansion (Δa) of the Straight SPAs is higher for all the cross-sectional geometries than their otherwise shaped counterparts. Although the differences among most of the SPAs results are small and could be neglected, it stands out the contrast between Straight and Helical/Pre-helical SPAs. A way to verify in more detail these values is by looking at the error bars in Fig. 6. In this figure, an SPA with high repeatability will show short or almost non-visible error bars.

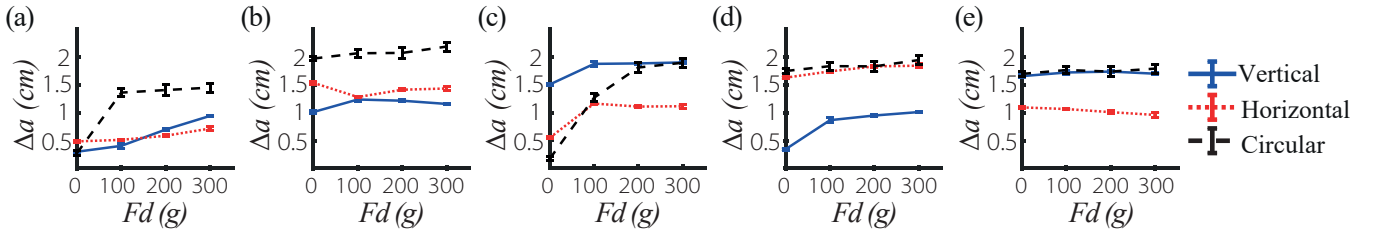


Fig. 6. Expansion performance of the SPAs across different chamber shapes and deflections under variable loading conditions (F_d): (a) Straight, (b) Curved, (c) Helical, (d) Pre-curved, (e) Pre-helical.

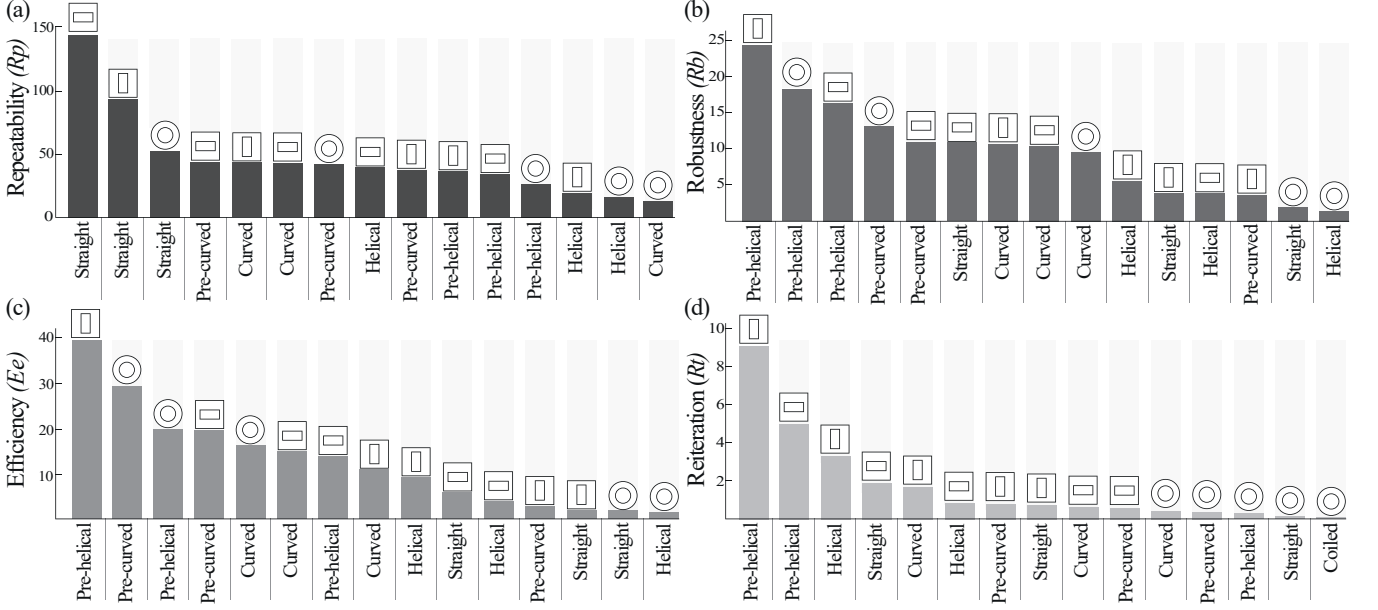


Fig. 7. SPAs reliability performance: (a) Repeatability, (b) Robustness, (c) Efficient expansion and (d) Reiteration.

2) *Robustness*: Fig.7 (b) shows a ranking of the SPAs from the highest to the lowest levels of robustness (R_b), showing the Vertical Pre-helical, Circular Pre-helical and Horizontal Pre-helical SPAs as the three most robust. By looking only at their chamber type, the Vertical Pre-helical, Circular Pre-curved, Vertical Helical, Vertical Curved and Straight Horizontal show the highest levels of robustness. A way to verify these values is by identifying the straightest lines on the x axis in Fig. 6.

3) *Expansion Efficiency*: Fig. 7(c) shows a ranking of the SPAs from the highest to the lowest efficiency (E_e), showing the Vertical Pre-helical, Circular Pre-curved and Circular Pre-helical SPAs as the three most efficient in terms of expansion. By segmenting the ranking based on chamber type, the SPAs with highest efficiency (E_e) are Vertical Pre-helical, Circular Pre-curved, Vertical Helical, Circular Curved and Horizontal Straight.

4) *Reiteration*: Fig. 7(d) shows a ranking of the SPAs from the highest to the lowest levels of reiteration (R_t). It shows that reiteration for the squared SPAs is higher than for their Circular counterparts. The difference between the first and last SPAs in the ranking is a standard deviation of ≈ 15 seconds, making it a highly relevant parameter to consider in the design of SPAs that may suffer variable

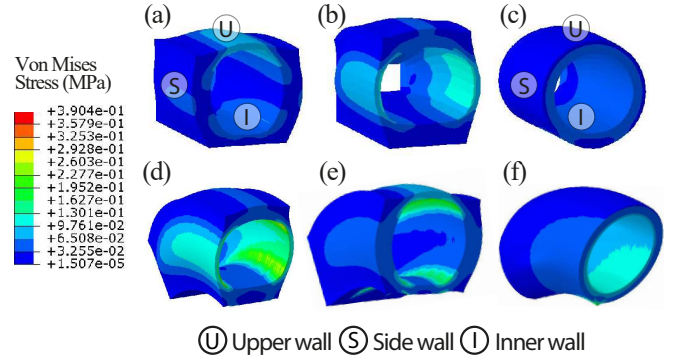


Fig. 8. Finite Element Analysis showing Von Mises stress contours of baseline Straight SPAs: (a) Horizontal, (b) Vertical, (c) Circular; and highly reliable SPAs per cross-sectional geometry based on the efficient Expansion (E_e) values (Fig. 7(c)): (d) Horizontal Pre-curved, (e) Vertical Pre-helical and (f) Circular Pre-curved.

loading conditions.

C. SPAs Stress Analysis

Fig. 8 and table II show the Von Mises stress concentration values obtained in the developed FEM for the Straight SPAs and their counterparts with the highest efficient expansion

TABLE II
VON MISES STRESS (KPA) CONCENTRATION VALUES IN FEM SPAS

SPA design	SPA Section		
	Inner Wall	Side Wall	Upper Wall
Horizontal Straight	32.55	0.01507	65.08
Vertical Straight	97.61	65.08	32.55
Circular Straight	32.55	0.01507	0.01507
Horizontal Pre-curved	260.3	97.61	32.55
Vertical Pre-helical	227.7	32.55	65.08
Circular Pre-curved	97.61	32.55	0.01507

(Ee) levels per cross-sectional geometry. For this study, we focused our analysis on three sections of the SPAs: (1) Inner wall; the inner wall measurements were taken from the areas where they are more prone to fail. In the square SPAs, the inner corners of the air channel and in the Circular SPAs, the area close to the fixed surface. (2) Side wall; for all the SPA designs, the side wall is the adjacent surface to the upper and lower face. (3) Upper Wall; the upper face is the opposite side to the fixed surface of the SPA, where the maximum expansion (Δa) (Fig. 3(d,e)) occurs.

Except for the upper face in Horizontal SPAs and the outer walls of Vertical SPAs, these values show an overall increment in stress in the non-straight squared SPAs. In the Circular Pre-curved SPA there is an increment in stress in the inner and outer wall. The upper face shows almost negligible amounts of stress for both Circular SPAs. Specifically, stress in the Horizontal Pre-curved SPA increases 700% and more than a thousand times on its inner and outer walls respectively, but in the upper wall it decreases by 50% in comparison to its Straight counterpart. For the Vertical Pre-Helical SPA, stress increases by 133% and 100% on its inner and upper walls respectively, but decreases by 50% in the outer wall in comparison to its Straight counterpart. In the Circular Pre-curved SPA, stress increases by 200% in the inner wall and more than thousand times in the outer wall. We can conclude that, Horizontal Pre-curved showed the highest increment and overall levels of stress, located in its inner and outer walls respectively, but Vertical Pre-helical showed the highest increment in its upper wall.

D. Statistical Analysis Results

1) *Significance of Cross-Sectional Geometry:* The test shows that there is overall statistically significant differences between the cross-sectional geometries of the chambers in relation to their average maximum expansion $\bar{\Delta a}$ (Fig. 9(a)). By conducting a *Post-Hoc* test, we identified that the statistically significant difference occurs specifically between the Circular and the two squared SPAs, but is not significant between the two squared SPAs, Horizontal and Vertical. This means that varying the orientation of the squared chambers does not impact the expansion of a SPA as much as using a Circular cross-section.

2) *Significance of Chamber Shape:* The test shows that there is overall statistically significant differences among the

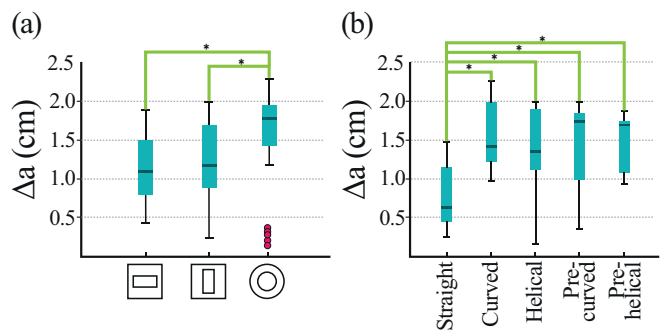


Fig. 9. Statistical Analysis Results for $\bar{\Delta a}$. (a) Significance among cross-sectional geometries. (b) Significance among SPAs chamber shapes.

chamber shapes in relation to $\bar{\Delta a}$ (Fig. 9(b)). By conducting a *Post-Hoc* test, we identified that the statistically significant difference occurs specifically between the Straight SPAs and the other chamber shapes. This means that using a Curved, Helical, Pre-curved or Pre-helical chamber shape will not impact the expansion of a SPA as much as using a Straight shape.

V. DISCUSSION

This work analyzes systematically the impact of deflection on the performance of SPAs with different chamber shapes and cross-sectional geometries under variable loading conditions to provide insights into the design of more reliable soft actuators. We selected actuators that are widely used in soft robotics based on their chamber shape (Straight, Curved, Helical, Pre-curved and Pre-helical) and cross-sectional geometries (Squared and Circular). Additionally, we implemented one variation orientation to capture its impact into their performance (Vertical and Horizontal). To provide a holistic comparative view on the behavior of the selected SPAs, we explored experimentally, numerically and statistically their differences in reliability, stress concentration and significance of expansion of geometry and shape.

While previous work addresses the reliability of soft actuators from a deterministic approach, they do not consider the influence of the variations in the chamber design, cross-sectional geometry and fabrication method triads, as well as dynamic factors such as deflections and pressurization, into the assessment of reliability of SPAs. Also, despite various efforts have been made to optimize different design parameters in SPAs design, the analysis is often focused on complex, constrained or reinforced examples that could be inadvertently hiding underlying effects of the SPAs alone.

A. Conditions that Impact on Reliability

All non-Straight SPAs showed lower levels of repeatability than their Straight counterparts. This can be explained by considering the viscoelasticity of silicone rubber and its effects as hysteresis, creep and stress relaxation, as well as considering elastic energy storage.

1) *Effects of Viscoelasticity:* Since elastomeric materials exhibit stress-strain characteristics that are time dependent, reiteration (Rt) values of the SPAs are affected by this

property. This is corroborated by Fig. 7(d), that shows time variation in reaching $\bar{\Delta}a$. Because a load is applied and sustained during the pressurization, we hypothesize that viscoelastic creep is affecting the robustness (Rb) and efficiency of expansion (Ee) of the SPAs, as seen in Fig. 7(b) and (c).

2) *Effects of Elastic Energy Storage and Chamber Shape:* In the case of non-Straight-deflected actuators (Curved and Helical SPAs), the deflection force needed to configure the actuator is stored as potential energy. This energy generates stress concentrations that might be affecting maximum expansion of the SPAs ($\bar{\Delta}a$). However, as demonstrated in [20], even a non-deflected non-Straight actuator (such as Pre-curved and Pre-helical SPAs) tends to straighten when it is pressurized also increasing stress concentrations (Fig. 8).

3) *Effects of Cross-sectional Geometry:* The cross-sectional geometry of the SPAs could potentially provide resistance to deflection, buckling and other mechanical instabilities. As shown in Fig. 2, the squared SPAs require more force to be deflected and to be buckled. This might explain their tolerance to external loads under the same loading conditions (Fd) and their reiteration (Rt) performance in comparison to the Circular SPAs. In summary, SPAs that can reduce the effects of viscoelasticity and energy storage due to their chamber shape and cross-sectional geometry produce highly reliable actuation. An example of this is the SPA Vertical Pre-helical, which showed to be the most reliable SPA as by showing the highest reiteration, robustness and efficiency. The implication is, that the height/width ratio of its cross-sectional geometry combined with its pre-shaped chamber shape mitigates better than the other SPAs the effects of viscoelasticity and the elastic energy stored into its structure. The relevance of the height/width ratio is visible as the Horizontal Pre-helical SPA was ranked in a lower position than the Vertical Pre-helical SPA for all the requirements (Fig. 7).

B. Statistical Analysis

The conducted statistical analysis concluded that the difference in maximum expansion between the squared and Circular SPAs is significant. The resistance of the SPAs to mechanical instabilities shows a similar conclusion (Fig. 2). This supports our previous assumption (Section V-A.3) on the effects of the cross-sectional geometry into the SPAs performance. The statistical analysis also concluded that the maximum expansion ($\bar{\Delta}a$) of Straight chambers is significantly different from all the other chamber shapes. This supports our assumptions on the effects of elastic potential energy (Section V-A.2). Although there is no significant difference among the maximum expansion ($\bar{\Delta}a$) of all the non-Straight SPAs and between Horizontal and Vertical SPAs, we recommend to select one or another chamber shape or geometry based on their final application and the corresponding confidence interval based on standardized metrics, such as safety factors, repeatability, robustness and reiteration.

C. Stress concentrations

The developed FEM highlights local stress concentrations that provide visualization of possible failure areas in the SPAs. It has been demonstrated that the geometry of the cross-section of a pneumatic chamber impacts on the stress distribution and consequently on global actuator performance [8]. In this paper, we demonstrated that the shape of the SPA also has an important impact on the stress concentration. In the presented scenarios, curving and coiling Straight SPAs with Horizontal, Circular and Vertical cross-sectional geometries increase the overall risk of failure. It is well known that rounded angles show higher average load carrying capacity than square right angles. In this study, we illustrated that by curving and coiling the Straight chambers. As a result, some sections of the SPAs increased in stress concentration by more than a thousand times (Section IV-C). We relate that increase to the effects of elastic energy storage described previously (Section V-A.2). Circular SPAs are more likely to fail in the areas close to the inextensible surface because its contact surface is reduced in comparison to the squared SPAs. However, despite its limitations in reliability, Circular SPAs show the lowest stress in their bodies, potentially allowing them to reach higher expansion rates without failing than their squared counterparts.

D. Design Principles

The results and analysis previously discussed in addition to supporting literature cited in Section I provide the basis for the following design principles of highly reliable SPAs.

1) *Straight SPAs yield higher repeatability than other deflected and pre-shaped SPAs:* Although the maximum deviation of expansion was 1 mm (Circular Helical SPA), there are tasks in which repeatability of expansion is non-trivial for the correct function of the system, as in surgical applications using laparoscopic instruments [26]. In these cases, Straight SPAs may provide better outcomes, specifically, Horizontal SPAs, which showed an average deviation of only 0.06mm. Nevertheless, it is important to consider the trade-off in efficiency. For instance, Circular Curved, which $\bar{\Delta}a$ is $> 300\%$ higher than for the most repeatable SPA, has an average deviation of only 0.72 mm, which could be enough if for example, it is implemented in an industrial soft gripper. We recommend to verify regulatory, operational and safety parameters that determine the degree of precision required by the system.

2) *Pre-shaped SPAs increase Efficiency in comparison to deflected SPAs:* Provided that deflections of the main body of the SPAs can be avoided, these will show overall higher efficiency than deflected SPAs. This can be confirmed by Fig. 7(c), where most of the pre-shaped SPAs are better ranked than the deflected SPAs. We assume that the reason for Vertical Pre-curved to be poorly ranked is the height-width ratio of the inner channel affecting its resistance to instabilities such as lateral-torsional buckling, and therefore, its performance. We suggest to keep the fabrication shape as close as possible to the final-use shape to avoid deflections that could be transformed into stored energy and residual

stress. An example of implementation of this principle is pure-motion actuators, as their extended, expanded or twisted configurations are often a scaled version of their relaxed state.

3) *Pre-helical SPAs increase robustness in comparison to Pre-curved and deflected SPAs:* Provided that the environment in which the actuator will perform and the application allows it, SPAs should be fabricated as Helical chambers. As can be seen in Fig. 7(b), the Pre-helical SPAs showed the highest robustness. Specifically, the Vertical Pre-helical SPA showed to have the highest robustness, which also showed high reiteration and the highest repeatability among the Pre-helical SPAs. As in the previous requirement, we assume that Vertical Pre-curved performance is affected by the height-width ratio of its inner channel. It is important to consider the trade-off regarding other reliability requirements. For example, in the case of the Circular Pre-helical, the second best SPA in robustness, it performs poorly in reiteration. We assume this happens due to the lower resistance of the Circular SPAs to mechanical instabilities. An example of the implementation of this principle is the design of actuators that have to carry variable loads. By using Pre-helical SPAs, they can lift these loads potentially minimizing variability of expansion.

4) *Straight Horizontal SPAs are potentially more reliable than traditional Straight Circular SPAs for axial deflections:* Straight SPAs that bend due to their inextensible layer can benefit from having a cross-sectional geometry as in the Horizontal SPA studied in this paper. Its efficiency and robustness is as optimal as the traditional Circular Curved SPA, but with a higher repeatability and reiteration. An example of implementation of this principle is the design of modular soft robots that use bending sections to steer their motion. By using Straight Horizontal SPAs with an inextensible layer, these robots can potentially follow a path with higher repeatability, efficiency and robustness than using any other SPA presented in this work.

VI. CONCLUSION

There has been a general oversight of a systematic design and performance analysis of SPA's as building blocks. Several publications [27], [26], [28], [9] have expressed a prevalent need to enhance soft robots reliability as a conduit for improved design, fabrication, modeling and control of these systems. In this article, we quantify the reliability performance of three SPA designs with different actuation response to deflection to provide a set of design principles that address the challenges of developing soft robots with predictable and reliable behaviour. We identified three main factors that impact SPAs reliable performance: (1) viscoelasticity of the SPAs' material, (2) elastic energy storage related to the SPAs chamber 3D shape and deflections and (3) the SPAs cross-sectional geometry. To overcome the negative effects of those factors such as low repeatability, time-wise inconsistent inflation and inefficient expansion, designers should select the optimal triad of cross-sectional geometry, chamber shape and fabrication method (deflected

or pre-shaped chambers) depending on the requirements of the system. By using the proposed rankings in Fig. 7 and applying the design principles into the development of soft robots, designers will be able to make informed decisions prior to the actuators fabrication. Although there can be a larger spectrum of chamber variations different from the SPAs presented within this work, the proposed methodology serves as a guideline for the assessment of most SPA design providing the soft robotics community with a useful tool for soft robots design. Further studies will include the development of a constitutive model for the prediction of the stress-strain relations, quantification of elastic potential energies to provide further depth into its effects on reliable performance and replication of the analysis to cover other SPA types, such as braided soft actuators.

ACKNOWLEDGMENTS

We thank Dr Nicolas Herzig and Joanna Jones for their input into the discussion about results implications.

REFERENCES

- [1] L. Qin, X. Liang, H. Huang, C. K. Chui, R. C.-H. Yeow, and J. Zhu, "A versatile soft crawling robot with rapid locomotion," *Soft robotics*, vol. 6, no. 4, pp. 455–467, 2019.
- [2] A. M. Nasab, A. Sabzehzar, M. Tatari, C. Majidi, and W. Shan, "A soft gripper with rigidity tunable elastomer strips as ligaments," *Soft robotics*, vol. 4, no. 4, pp. 411–420, 2017.
- [3] A. T. Asbeck, S. M. De Rossi, I. Galiana, Y. Ding, and C. J. Walsh, "Stronger, smarter, softer: next-generation wearable robots," *IEEE Robotics & Automation Magazine*, vol. 21, no. 4, pp. 22–33, 2014.
- [4] E. Perez-Guagnelli, J. Jones, A. H. Tokel, N. Herzig, B. Jones, S. Miyashita, and D. D. Damian, "Characterization, simulation and control of a soft helical pneumatic implantable robot for tissue regeneration," *IEEE Transactions on Medical Robotics and Bionics*, vol. 2, no. 1, pp. 94–103, 2020.
- [5] J. Kim, J. W. Kim, H. C. Kim, L. Zhai, H.-U. Ko, and R. M. Muthoka, "Review of soft actuator materials," *International Journal of Precision Engineering and Manufacturing*, pp. 1–21, 2019.
- [6] K. Suzumori, S. Endo, T. Kanda, N. Kato, and H. Suzuki, "A bending pneumatic rubber actuator realizing soft-bodied manta swimming robot," in *Proceedings 2007 IEEE International Conference on Robotics and Automation*. IEEE, 2007, pp. 4975–4980.
- [7] K. Ogura, S. Wakimoto, K. Suzumori, and Y. Nishioka, "Micro pneumatic curling actuator-nematode actuator," in *2008 IEEE International Conference on Robotics and Biomimetics*. IEEE, 2009, pp. 462–467.
- [8] P. Polygerinos, Z. Wang, J. T. Overvelde, K. C. Galloway, R. J. Wood, K. Bertoldi, and C. J. Walsh, "Modeling of soft fiber-reinforced bending actuators," *IEEE Transactions on Robotics*, vol. 31, no. 3, pp. 778–789, 2015.
- [9] J. Zhang, T. Wang, J. Wang, M. Y. Wang, B. Li, J. X. Zhang, and J. Hong, "Geometric confined pneumatic soft-rigid hybrid actuators," *Soft Robotics*, 2020.
- [10] I. De Falco, M. Cianchetti, and A. Menciassi, "A soft multi-module manipulator with variable stiffness for minimally invasive surgery," *Bioinspiration & biomimetics*, vol. 12, no. 5, p. 056008, 2017.
- [11] K. Bertoldi, V. Vitelli, J. Christensen, and M. van Hecke, "Flexible mechanical metamaterials," *Nature Reviews Materials*, vol. 2, no. 11, pp. 1–11, 2017.
- [12] G. Miron and J.-S. Plante, "Design principles for improved fatigue life of high-strain pneumatic artificial muscles," *Soft Robotics*, vol. 3, no. 4, pp. 177–185, 2016.
- [13] J. Yan, X. Zhang, B. Xu, and J. Zhao, "A new spiral-type inflatable pure torsional soft actuator," *Soft robotics*, vol. 5, no. 5, pp. 527–540, 2018.
- [14] M. A. Robertson, H. Sadeghi, J. M. Florez, and J. Paik, "Soft pneumatic actuator fascicles for high force and reliability," *Soft robotics*, vol. 4, no. 1, pp. 23–32, 2017.

- [15] R. V. Martinez, A. C. Glavan, C. Keplinger, A. I. Oyetibo, and G. M. Whitesides, "Soft actuators and robots that are resistant to mechanical damage," *Advanced Functional Materials*, vol. 24, no. 20, pp. 3003–3010, 2014.
- [16] A. Al-Ibadi, S. Nefti-Meziani, and S. Davis, "Novel models for the extension pneumatic muscle actuator performances," in *2017 23rd international conference on automation and computing (ICAC)*. IEEE, 2017, pp. 1–6.
- [17] J. Yan, H. Dong, X. Zhang, and J. Zhao, "A three-chambered soft actuator module with omnidirectional bending motion," in *2016 IEEE International Conference on Real-time Computing and Robotics (RCAR)*. IEEE, 2016, pp. 505–510.
- [18] F. Connolly, C. J. Walsh, and K. Bertoldi, "Automatic design of fiber-reinforced soft actuators for trajectory matching," *Proceedings of the National Academy of Sciences*, vol. 114, no. 1, pp. 51–56, 2017.
- [19] M. Calisti, M. Giorelli, G. Levy, B. Mazzolai, B. Hochner, C. Laschi, and P. Dario, "An octopus-bioinspired solution to movement and manipulation for soft robots," *Bioinspiration & biomimetics*, vol. 6, no. 3, p. 036002, 2011.
- [20] A. Pal, D. Goswami, and R. V. Martinez, "Elastic energy storage enables rapid and programmable actuation in soft machines," *Advanced Functional Materials*, p. 1906603, 2019.
- [21] H. Takeshima and T. Takayama, "Geometric estimation of the deformation and the design method for developing helical bundled-tube locomotive devices," *IEEE/ASME Transactions on Mechatronics*, vol. 23, no. 1, pp. 223–232, 2017.
- [22] F. Connolly, P. Polygerinos, C. J. Walsh, and K. Bertoldi, "Mechanical programming of soft actuators by varying fiber angle," *Soft Robotics*, vol. 2, no. 1, pp. 26–32, 2015.
- [23] F. Ilievski, A. D. Mazzeo, R. F. Shepherd, X. Chen, and G. M. Whitesides, "Soft robotics for chemists," *Angewandte Chemie International Edition*, vol. 50, no. 8, pp. 1890–1895, 2011.
- [24] E. R. Perez-Guagnelli, S. Nejus, J. Yu, S. Miyashita, Y. Liu, and D. D. Damian, "Axially and radially expandable modular helical soft actuator for robotic implantables," in *2018 IEEE International Conference on Robotics and Automation (ICRA)*. IEEE, 2018, pp. 1–9.
- [25] G. Agarwal, N. Besuchet, B. Audergon, and J. Paik, "Stretchable materials for robust soft actuators towards assistive wearable devices," *Scientific reports*, vol. 6, no. 1, pp. 1–8, 2016.
- [26] M. Runciman, A. Darzi, and G. P. Mylonas, "Soft robotics in minimally invasive surgery," *Soft robotics*, vol. 6, no. 4, pp. 423–443, 2019.
- [27] R. S. Diteesawat, T. Helps, M. Taghavi, and J. Rossiter, "Characteristic analysis and design optimization of bubble artificial muscles," *Soft Robotics*, 2020.
- [28] C. Laschi, J. Rossiter, F. Iida, M. Cianchetti, and L. Margheri, "Soft robotics: Trends, applications and challenges," *Livorno, Italy*, 2016.